Materials Chemistry and Physics 111 (2008) 375–380

Contents lists available at ScienceDirect

Materials Chemistry and Physics

journal homepage: www.elsevier.com/locate/matchemphys

Interface microstructure study of friction stir lap joint of AC4C cast aluminum alloy and zinc-coated steel

Y.C. Chen [a,*], T. Komazaki [b], Y.G. Kim [a], T. Tsumura [a], K. Nakata [a]

[a] Joining and Welding Research Institute, Osaka University, 11-1 Mihogaoka, Ibaraki, Osaka 567-0047, Japan
[b] Ryobi Limited, 5-2-8 Toshima, Kita-ku, Tokyo 114-8518, Japan

ARTICLE INFO

Article history:
Received 14 March 2007
Received in revised form 27 March 2008
Accepted 17 April 2008

Keywords:
Welding
Alloys
Mechanical properties
Microstructure

ABSTRACT

AC4C cast Al alloy and zinc-coated steel are successfully lap jointed using friction stir welding. The interface microstructure is investigated using optical microscopy, scanning electron microscopy and X-ray diffraction. The mechanical properties of the joints are evaluated using tensile test. Experimental results show that the lap joint consisted of four part structures, i.e. stir zone structure of Al alloy, new intermetallic compounds layer, old intermetallic compounds layer of original zinc coat and base material of steel. The thickness of intermetallic compounds layer increases with decreasing welding speeds and has a significant effect on the strengths of the joints. Heavy thickness of intermetallic compounds layer seriously deteriorates the mechanical properties of the joints. The intermetallic compounds layer mainly contains Fe_2Al_5 and Fe_4Al_{13}.

1. Introduction

Aluminum alloys with high strength, good formability and weight saving are being considered for fabrication of vehicles. Zinc-coated steel with excellent corrosion resistance and good durability is a promising structural material in vehicle applications [1,2]. In order to achieve combined properties of aluminum alloys and zinc-coated steel, development of reliable joints between aluminum alloy and zinc-coated steel is necessary. However, most studies to date mainly focus on dissimilar metal joining of aluminum alloy and steel [3–8] and few researches involve joining aluminum alloy and zinc-coated steel [9]. From the industrial application point of view, developing adaptive joining method for welding aluminum alloy and zinc-coated steel is in urgent need.

Friction stir welding (FSW) is a new joining process invented at The Welding Institute (TWI) in 1991. The most attractive aspect for the novel joining technology is that the base materials are not melted during the welding. Therefore, the porosity and grain boundary cracking can be eliminated and the mechanical properties of the joints can be significantly improved. People also look forward to obtaining such advantages for joining dissimilar materials using FSW technology [10–17]. Ahmed et al. have invested the weldabilities of 1100H24 and Zn-coated steel using friction stir welding [9]. They find that the performance of the joint depends strongly on the depth of the probe tip of the friction stir-welding tool into the steel surface. When the probe depth does not reach the steel surface the joint shows quite weak fracture loads, while the penetration of the probe tip to a depth of 0.1 mm under the steel surface significantly increases the joint strength [9]. However, when the tool is inserted into the steel base material, the tool is seriously worn. In order to increase the service life of the tool for friction stir welding, special materials for the tool should be selected. It was well known that the tools for friction stir welding of high temperature material such as PCBN, W–Re alloy are expensive. In this study, AC4C cast aluminum alloy and low carbon zinc-coated steel are selected as the experimental materials for friction stir lap welding. The aluminum alloy plate was put on the zinc-coated steel plate. The inserting depth is strictly controlled less than the thickness of the aluminum alloy. The emphasis is placed on the interface microstructure evolution of the welds.

2. Experimental

The base material used in this study was a 3-mm-thick AC4C cast aluminum alloy plate and a 0.8-mm-thick low carbon zinc-coated steel plate. The plate was cut and machined into rectangular welding samples, 300 mm long by 100 mm wide, and they were lap-welded using an FSW machine. The relative position of aluminum alloy and zinc-coated steel in transverse direction is shown in Fig. 1. The welding parameters are rotation speed of 1500 rpm and welding speed of 60–120 mm min^{-1}. The upsetting force of the welding tool (SKD61 tool steel) used in this experiment is 9.8 kN. Position control mode is used in this experiment and the insert depth of tool is 2.9 mm. The shoulder diameter and probe diameter of the tool are 15 mm and 5 mm, respectively. The length of the probe is 2.9 mm and the welding tilt angle is 3°.

After welding, the joint was cross-sectioned perpendicular to the welding direction for metallographic analyses and tensile tests using an electrical-discharge

* Corresponding author. Tel.: +81 6 6879 8668; fax: +81 6 6879 8668.
E-mail address: armstrong@hit.edu.cn (Y.C. Chen).

0254-0584/$ – see front matter © 2008 Elsevier B.V. All rights reserved.
doi:10.1016/j.matchemphys.2008.04.038

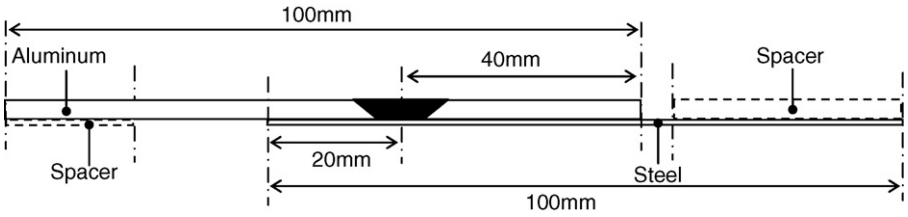

Fig. 1. A schematic plan of the relative position of aluminum alloy and steel.

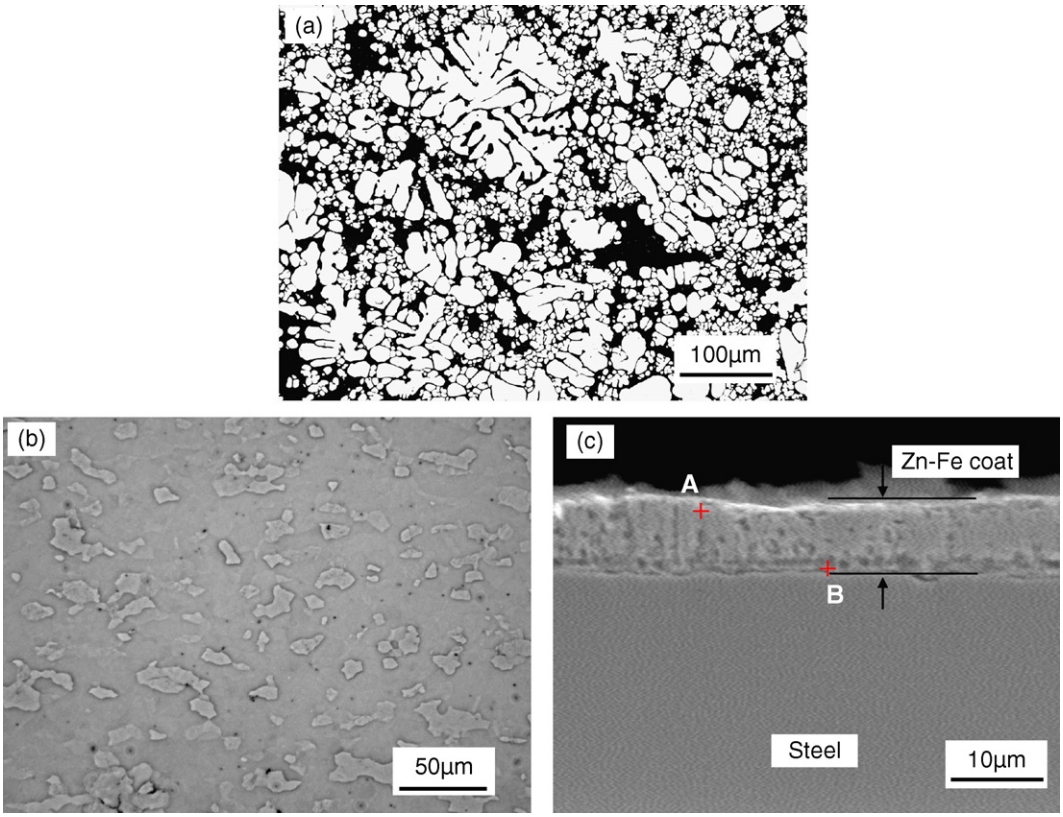

Fig. 2. Microstructure of the base material: (a) AC4C aluminum alloy, (b) steel, and (c) zinc coat.

cutting machine. The cross-sections of the metallographic specimens were polished with diamond polishing agent, etched with Keller's reagent (1 ml hydrochloric acid, 1.5 ml nitric acid, 2.5 ml hydrofluoric acid and 95 ml water) and observed by optical microscopy.

The mechanical properties of the joint were measured using tensile tests. The tensile tests were carried out at room temperature at a crosshead speed of 1 mm min^{-1} using a tensile testing machine, and the mechanical properties of the joint were evaluated using three tensile specimens cutting from the same joint. The shape of the test specimen is rectangular and the width of each specimen is 20 mm. The typical cross-section of tensile specimens is the same with that shown in Fig. 1.

The interface structure and element distribution in the weld were analyzed by scanning electron microscopy (SEM) equipped with an energy-dispersive X-ray (EDX) spectroscopy analysis system. The phase structure on the surface of fracture of the joints was determined using X-ray diffraction (XRD).

3. Results and discussion

Fig. 2 shows the microstructure of the base materials. AC4C base material is a hypoeutectic Al–Si alloy (see Table 1), therefore the base material presents typical hypoeutectic structure (see Fig. 2a). The steel base material shows ferritic structure due to low carbon content (see Fig. 2b). Fig. 2c shows the microstructure near the zinc coat surface. It can be seen from this figure that the thickness of Zn coat is about 10 μm. The Zn coat is composed of iron–zinc intermetallic compounds since it is produced using hot-dip galvanizing process. Elements analysis results show that the intermetallic compounds mainly forms at the interface of Zn coat and steel. The chemical composition (at.%) of points A and B

Table 1
Chemical compositions and mechanical properties of base materials

Base materials	Chemical compositions (mass%)										Mechanical properties	
	Al	Cu	Mn	Fe	C	Mg	Ni	P	Si	S	Strength (MPa)	Elongation (%)
AC4C	Bal.	0.05	0.3	0.15	–	0.2	–	–	7.5	–	244	7.4
Zn-coated steel	0.06	0.02	0.20	Bal.	0.04	–	0.01	0.013	–	0.005	328	33.4

Table 2
Tensile properties and fracture locations of the joints

Parameters	60 mm min^{-1}	80 mm min^{-1}	100 mm min^{-1}	120 mm min^{-1}
Strength	50.1 MPa	321.7 MPa	331.8 MPa	330.9 MPa
Fracture location	Interface	Steel base material	Steel base material	Steel base material

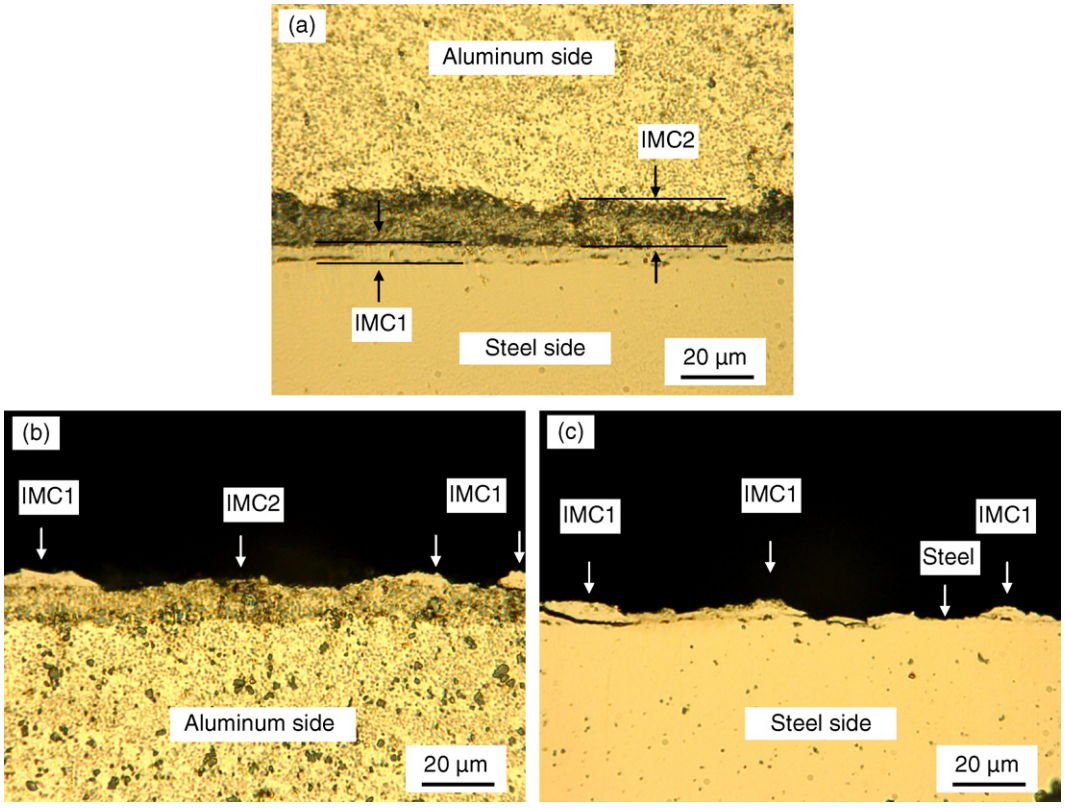

Fig. 3. Fracture location of the joint (60 mm min^{-1}): (a) before tensile test, (b) aluminum side after tensile test, and (c) steel side after tensile test.

are 75.06%Zn–20.73%Fe–4.21%Al and 62.91%Zn–34.95%Fe–2.15%Al, respectively. From these analysis results and Fe–Zn binary diagram it can be determined that the interface involves Fe–Zn intermetallic compounds. The contents of zinc increase when approaching the surface of layer. That is to say, the composition of layer gradually approaches pure zinc from the interface to the surface.

Table 2 shows tensile test results of the joints with different welding parameters. Experimental results show that welding speed has a significant effect on tensile strengths and fracture locations of the joints at the rotation speed of 1500 rpm. When welding speed is higher than 80 mm min^{-1}, the joints fracture in the zinc-coated steel base material and the tensile strength of the joint is equal to that of zinc-coated steel. When the welding speed is 60 mm min^{-1}, the joints fracture in the interface of the weld and the shear strength is about 50 MPa. In order to further determine the fracture mechanism of the joint, the microstructure observation of the fracture location of the joint is carried out. Fig. 3 shows the cross section of the joint before and after tensile test. It can be seen from Fig. 3a that the joint consists of four layers structure, i.e. stir zone structure of Al alloy, IMC2, IMC1 and base material of steel. Interface microstructure observation from base metal to weld center shows that partial original zinc coat remains after welding. For convenience's sake, the remaining zinc coat layer is called IMC1 in this paper. Between the IMC1 layer and stir zone structure of Al alloy, there is a new IMC2 layer produced during welding. That is to say, after welding the partial original rich-zinc coat is replaced by new IMC2 layer. Fig. 3b and c shows the cross section of the joint after tensile test. It shows clearly that the joint fractures at the interface between IMC1 and IMC2 layer. Moreover, we can know that the cohesion between stir zone structure of Al alloy and IMC2 layer is higher than that between IMC1 and IMC2 layer. Some fragments of broken IMC1 layer were clayed on the surface of IMC2 layer. From Fig. 3c we can know that IMC1 layer was seriously damaged during tensile test. Partial fracture happens at the interface between IMC1 layer and steel base material.

In order to determine the intermetallic compounds composition in the interface, map scanning and elements analysis to the interface structure are carried out near the interface. Experimental results are shown in Fig. 4 and Table 3. Fig. 4 illustrates the representative concentration profiles of Al, Si, Zn and Fe cross the interface

Table 3
Elements analysis results of the interface layer

Position	Element (mass%)			
	Al	Fe	Zn	Si
A	78.86	8.38	1.15	11.62
B	43.84	14.72	10.3	31.40
C	52.65	25.36	12.71	9.28
D	47.07	37.59	7.62	7.73
E	14.84	83.38	0.6	1.18
Original zinc coat	1.59	20.28	78.13	–

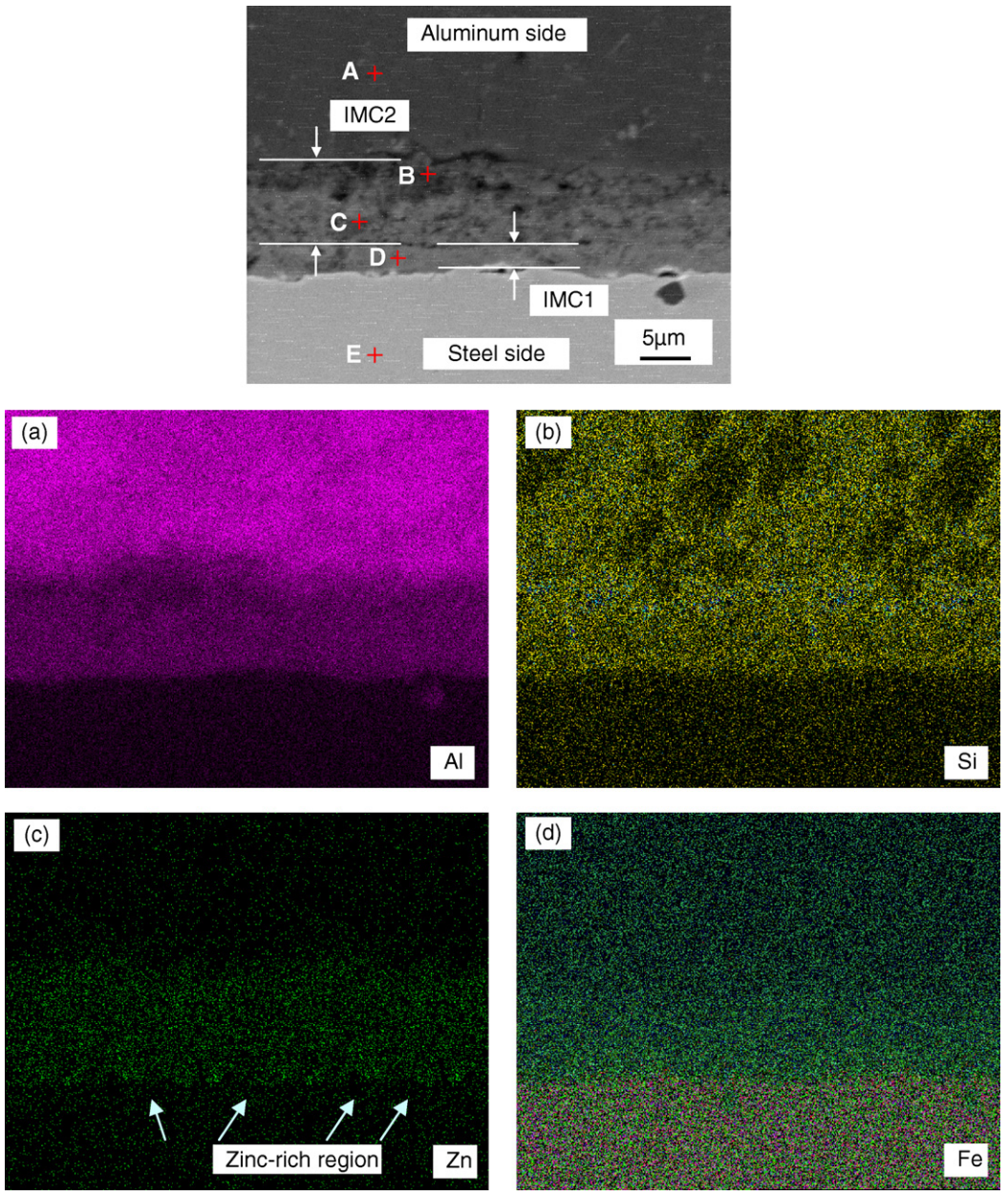

Fig. 4. Microstructure analysis of the interface layer: (a) SEM image, (b) map scanning of Al, (c) map scanning of Si, and (d) map scanning of Fe.

between base steel and aluminum alloy. A layer involving Al, Fe, Zn and Si forms at the interface of the joint as shown in Fig. 4. The elements analysis results of the Al–Fe–Si–Zn layer and the adjacent region are shown in Table 3. From these analysis results and Fe–Al binary diagram and Fe–Al–Zn ternary diagram we can know that the layer possibly involves Al, Fe, Al–Fe or Al–Fe–Zn intermetallic compounds. Moreover, it can be found from SEM image that some original intermetallic compounds of IMC1 remain at the interface between the steel base material and IMC2 layer. That is to say, aluminum alloy and steel are joined through intermediate reaction zone. Therefore, it is inevitable that the distribution characteristics of intermetallic compounds will affect the mechanical properties of the lap joint. Fig. 5 shows the relationship between IMC thickness and welding speeds. The measurement results of IMC thickness show that the thickness of the IMC significantly increases from 7.7 μm to 58.1 μm with welding speeds decreasing from 120 mm min^{-1} to 60 mm min^{-1}. Lower welding speed means

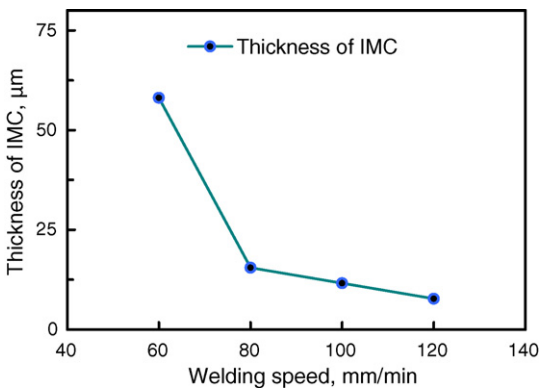

Fig. 5. Thickness of IMC changed with welding speeds.

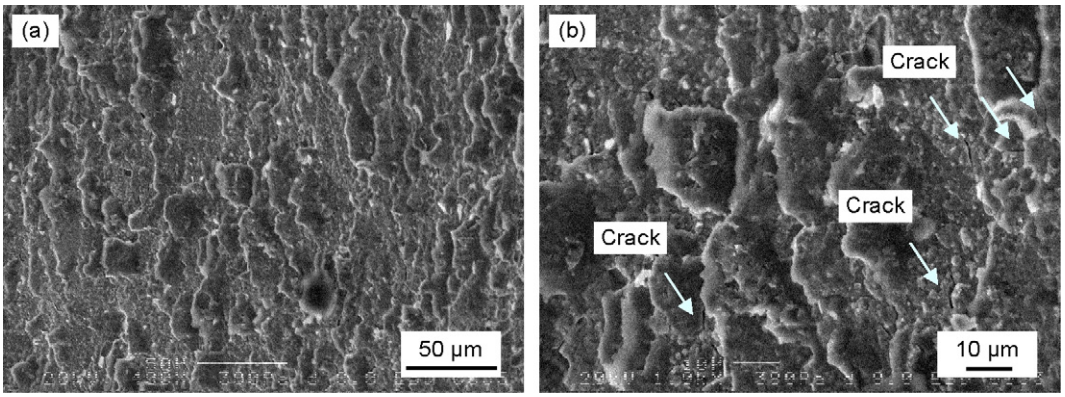

Fig. 6. Fracture characteristic of the joint: (a) low magnification image and (b) high magnification image.

higher welding heat input and longer holding time. Namely, the reaction at interface sufficiently takes place at a lower welding speed, which leads to heavy thickness of IMC. Heavy thickness of IMC increases brittleness of the lap joint and leads to the change of the weakest part of the joint from thin steel plate to the interface.

SEM micrographs of the fracture surface from aluminum side are shown in Fig. 6. Fig. 6b is the magnification of Fig. 6a. The fracture surfaces are mainly composed of brittle fracture with some micro cracks. This indicates that the intermetallic compounds layer at the interface is brittle. When the thickness of the interface increases to a certain degree, heavy thickness of intermetallic compounds leads to the change of the weakest part of the joint from thin steel plate to the interface.

In order to further determine if the intermetallic compounds form at the interface, X-ray diffraction patterns from fractured surfaces of the aluminum and steel sides are analyzed. XRD analysis results from the fractures are shown in Fig. 7. Diffraction lines that are attributable to intermetallic compounds of Fe_2Al_5 and Fe_4Al_{13} are at detected both aluminum side and steel side. At the same time, elements of Si, Al and Fe are also found out and no Al–Fe–Zn intermetallic compounds are detected. In the phase diagram of an Al–Fe system, there are several iron aluminide intermetallic compounds, such as Fe_3Al, FeAl, $FeAl_2$, Fe_2Al_5 and Fe_4Al_{13}. First phase to form under this kind of solid–solid interaction can be predicted by effective heat of formation (EHF) theory proposed by Pretorius et al. [18–20]. According to this theory, the first phase that forms during metal–metal interaction is the phase with the most negative heat of formation at the concentration of the lowest eutectic of the binary system. Furthermore, these phases react with each other to form a phase with a composition between that of the interacting phases and closest to that of the lowest eutectic composition. Al–Fe binary phase diagram has the lowest eutectic at 0.02% Fe. At this composition, the effective free energy of formation has been calculated at 773 K [21]. These results show that Fe_4Al_{13} has the lowest effective free energy of formation. It shows that the formation of Fe_4Al_{13} phase is kinetically favored. In the later stage, Fe_4Al_{13} and Fe phases will react with each other to form a phase with a composition between that of the interacting phases and closest to that of the lowest eutectic composition, i.e. Fe_2Al_5.

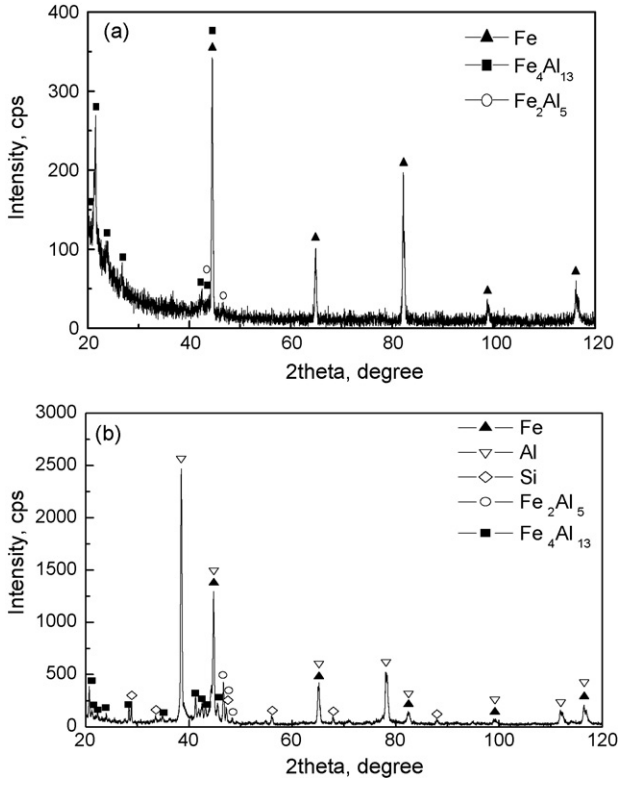

Fig. 7. XRD analysis results: (a) steel side and (b) aluminum side.

4. Conclusion

The sound lap joints of AC4C cast aluminum alloy and zinc-coated steel have been successfully obtained even when the inserting depth of the tool is less than the thickness of the aluminum alloy. The main results are shown as followed:

1. The lap joint consists of four part structures, i.e. stir zone structure of aluminum alloy, new intermetallic compounds layer, old intermetallic compounds layer of original zinc coat and base material of steel. Aluminum alloy and steel are joined through intermediate reaction zone.
2. Welding speeds have a significant effect on the mechanical properties of the joints at the rotation speed of 1500 rpm. When the welding speed is higher than 80 mm min^{-1}, the joints fracture in the zinc-coated steel base material and the tensile strength of the joint is equal to that of the zinc-coated steel. When the welding speed is 60 mm min^{-1}, the joints fracture in the interface of the weld and the shear strength is about 50 MPa. The joint fractures at the interface between new intermetallic compounds layer and old intermetallic compounds layer of original zinc coat.
3. Intermetallic compounds of Fe_2Al_5 and Fe_4Al_{13} are detected in joining interface.

References

[1] G. Kobe, Chilton's Auto. Ind. 7 (1994) 44.
[2] S. Ramasamy, Weld. J. 2 (2003) 35.
[3] J. Tsujino, K. Hidai, A. Hasegawa, R. Kanai, H. Matsuura, K. Matsushima, T. Ueoka, Ultrasonics 40 (2002) 371.
[4] M.U. Kamachi, R.B. Ananda, K. Shanmugam, R. Natarajan, B. Raj, J. Nucl. Mater. 321 (2003) 40.
[5] K. Matsugi, Y. Wang, T. Hatayama, O. Yanagisawa, K. Syakagohri, J. Mater. Proc. Technol. 135 (2003) 75.
[6] W.B. Lee, Y.M. Yeon, D.U. Kim, S.B. Jung, Mater. Sci. Technol. 19 (2003) 773.
[7] K. Kimapong, T. Watanabe, Weld. J. 83 (2004) 277.
[8] T. Murakami, K. Nakata, H. Tong, M. Ushio, Iron Steel Inst. Jpn. Inter. 43 (2003) 1596.
[9] E. Ahmed, T. Makoto, I. Kenji, Quart. J. Jpn. Weld. Soc. 23 (2005) 186.
[10] W.B. Lee, S.B. Jung, Mater. Res. Innovat. 8 (2004) 93.
[11] L.E. Murr, R.D. Flores, O.V. Flores, J.C. McClure, G. Liu, D. Brown, Mater. Res. Innovat. 1 (1998) 211.
[12] L.E. Murr, Y. Li, E.A. Trillo, J.C. McClure, Mater. Technol. 15 (2000) 37.
[13] L.E. Murr, Y. Li, R.D. Flores, E.A. Trillo, J.C. McClure, Mater. Res. Innovat. 2 (1998) 150.
[14] J. Yan, Z. Xu, Z. Li, L. Li, S. Yang, Scripta Mater. 53 (2005) 585.
[15] Y.S. Sato, S.H.C. Park, M. Michiuchi, H. Kokawa, Scripta Mater. 50 (2004) 1233.
[16] A.C. Somasekharan, L.E. Murr, Mater. Character. 52 (2004) 49.
[17] W.B. Lee, Y.M. Yeon, S.B. Jung, Scripta Mater. 49 (2003) 423.
[18] R. Pretorius, A.M. Vredenberg, F.W. Saris, J. Appl. Phys. 70 (1991) 3636.
[19] R. Pretorius, R. de Reus, A.M. Vredenberg, F.W. Saris, Mater. Lett. 9 (1990) 494.
[20] R. Pretorius, Vacuum 41 (1990) 1038.
[21] I. Ansara, T. Dinsdale, M.H. Rand (Eds.), Thermochemical Database for Light Metal Alloys, vol. 2, COST, Luxembourg, 1998, p. 23.